Journal of Electroceramics, 9, 209–214, 2002
© 2003 Kluwer Academic Publishers. Manufactured in The Netherlands.

The Effects of Lithium and Oxygen Contents Inducing Capacity Loss of the $LiMn_2O_4$ Obtained at High Synthetic Temperature

YUN SUNG LEE,[1] YASUFUMI HIDESHIMA,[2] YANG KOOK SUN[3] & MASAKI YOSHIO[1,*]

[1]*Department of Applied Chemistry, Saga University, 1 Honjo, Saga 840-8502, Japan*
[2]*Industrial Technology Center of Saga, 114 Yaemizo Nabeshima-cho, Saga 849-0932, Japan*
[3]*Department of Chemical Engineering, Hanyang University, 17 Haengdang-dong, Seoul 133-791, Korea*

Submitted August 28, 2002; Revised October 30, 2002; Accepted January 4, 2003

Abstract. Well-crystallized $LiMn_2O_4$ has been synthesized at different calcination temperatures using the melt-impregnation method. The lattice constant of $LiMn_2O_4$ increased with increasing calcination temperatures. $Li/LiMn_2O_4$cells calcined at lower temperatures (700–800°C) showed excellent cycling performances at room temperature. However, those cells calcined at higher temperature (850–900°C) exhibited abrupt capacity loss in the early stage and very poor cycle retention rate (<65%) after 50 cycles. It was considered that poor cycle performance of the spinels obtained at high temperature resulted from the lithium sublimation and oxygen deficiency during synthetic process. We found that above two factors, lithium sublimation and oxygen deficiency, were the commonly important factors to induce capacity loss in the $Li/LiMn_2O_4$ system, especially obtained at high synthetic temperature.

Keywords: $LiMn_2O_4$, spinel, lithium sublimation, oxygen deficiency, lithium battery

Introduction

Spinel $LiMn_2O_4$ and the layered $LiMnO_2$(M = Co, Ni, Mn) materials are the most widely studied 4 V cathode materials for lithium secondary batteries [1–8]. Among those, $LiMn_2O_4$ spinel has been extensively investigated as the most promising a cathode material for lithium secondary batteries because of its low cost, easy preparation, and environmental advantage [5–8].

$LiMn_2O_4$ has a cubic spinel structure with a space group $Fd\bar{3}\,m$ symmetry in which the Li^+ and $Mn^{3+/4+}$ ions are located at the 8a tetrahedral sites and the 16d octahedral sites of the structure, respectively. Although the cubic structure of the spinel is maintained during the insertion/extraction of Li^+ ions in the 4 V region, it still shows a small capacity loss on cycling at both room and high temperatures. The main capacity loss mechanism of the $LiMn_2O_4$ electrode in the 4 V region has been suggested as follows: (1) the slow dissolution of $LiMn_2O_4$ electrode in the electrolyte by a disproportination reaction ($2Mn^{3+} \rightarrow Mn^{4+} + Mn^{2+}$) [9], (2) unstable two-phase region in high voltage regions [10], (3) electrolyte decomposition at high potentials [11], and (4) Jahn-Teller distortion in the deeply discharged state [12].

Recently, Xia and Yang et al. have been reported the correlating capacity fading and structural changes in the $Li_{1+y}Mn_2O_{4-\delta}$ spinel system. They accurately controlled the composition of the $LiMn_2O_4$ spinel between 700–800°C for 24 h in air or N_2 flow [13, 14]. From the in-situ XRD and cycling curves, they found that both the charge/discharge profile and the structural changes in the $LiMn_2O_4$ spinel during cycling are very closely related to the oxygen deficiency degree. They suggested that a higher degree of oxygen deficiency is accompanied by a faster capacity fading during cycling.

Based on previous reports [1–14], we believe that lithium amount and oxygen content should be considered as important key parameters for inducing capacity loss of $LiMn_2O_4$ calcined at higher temperature. Specially, $LiMn_2O_4$ obtained at high temperature (≥850°C) showed a poor cycle characterization which resulted from lithium sublimation at high synthetic temperature. This indication was well explained that

*To whom all correspondence should be addressed.

a small extra amount of lithium should be added to supply for the lithium deficiency of $LiMn_2O_4$.

Therefore, we adopted the Xia's concept [14] in this study, which was a trial to reveal the effect of oxygen deficiency in the well-optimized $LiMn_2O_4$ spinel. In order to investigate simultaneously both the lithium and oxygen effects on the electrochemical properties of the $LiMn_2O_4$, these spinels were calcined at various calcination temperatures (700–900°C). The constants in this study were the fixed Li/Mn (1:1) ratio of starting materials, which differ from those of Xia's obtained at various lithium contents, to investigate the change in the lithium content in the spinel structure due to the sublimation of lithium as well as the effect of the oxygen deficiency at high temperature. We also introduce here the unique analysis method of oxygen content and its role of capacity loss mechanism in $Li/LiMn_2O_4$ system.

Experimental

$LiMn_2O_4$ compounds were synthesized using $LiOH \cdot H_2O$ (Katayama Chemical, Japan) and Mn_3O_4 (Tosoh Chemical, Japan) by the melt-impregnation method. The stoichiometric amount mixture of LiOH and Mn_3O_4 source was precalcined at 470°C for 10 h in O_2 and then postcalcined at desirable temperatures (700–900°C) for 20 h in air. The powder X-ray diffraction (XRD, Rint 1000, Rigaku, Ltd., Japan) using Cu K_α radiation was employed to identify the crystalline phase of the synthesized material. Rietveld refinement analysis was performed with XRD data to obtain the lattice parameters. The contents of Li and Mn in the resulting materials were analyzed with an inductively coupled plasma spectrometer (ICP, SPS7800, Seiko Instrument, Japan) by dissolving the powder in the dilute nitric acid. Oxygen content was measured quantitatively using an oxygen determination analyzer (RO-416DR, EF-40C, LECO Corporation, USA). In order to calculate the average Mn oxidation state, titration with excess $FeSO_4$ solution with standard $KMnO_4$ solution was carried out. The total Mn ion was determined by a complexometric titration method, in which excess EDTA was analyzed by back titration using standard zinc solution. The sample was first dissolved in hydroxylammonium chloride solution containing EDTA in advance.

The electrochemical characterizations were performed using CR2032 coin-type cells. The cathode was fabricated with 20 mg of accurately weighed active material and 12 mg of conductive binder (8 mg of Teflonized acetylene black (TAB) and 4 mg of graphite). It was pressed on 200 mm^2 stainless steel mesh used as the current collector under a pressure of 300 kg/cm^2 and dried at 200°C for 5 h in an oven. The test cell was made of a cathode and a lithium metal anode (Cyprus Foote Mineral Co.) separated by a porous polypropylene film (Celgard 3401). The electrolyte used was a mixture of 1M $LiPF_6$-ethylene carbonate (EC)/dimethyl carbonate (DMC) (1:2 by vol., Ube Chemical, Japan). The charge and discharge current density was 0.4 mA/cm^2 with a cutoff voltage of 3.0 to 4.3 V.

Results and Discussion

Figure 1 shows the X-ray diffraction (XRD) patterns of the $LiMn_2O_4$ compounds using LiOH and Mn_3O_4 as starting materials calcined at various synthetic temperatures (700–900°C). It was confirmed that the $LiMn_2O_4$ spinels have a cubic unit cell with a $Fd\bar{3}\ m$ space group in all temperature regions. There are no impurity peaks such as MnO_2, Mn_2O_3, and Li_2MnO_3, which were often found in other reports using the conventional solid-state method. Yamada et al. already reported the synthesis of $LiMn_2O_{4\pm\delta}$ materials at various calcination temperatures using a quenching technique [15]. Even though they succeeded in synthesizing a single $LiMn_2O_4$ spinel phase in the lower temperature region (<836°C), they found that the typical two-phase reaction occurred in the $LiMn_2O_4$ spinel structure, which changed the volume ratios between the cubic spinel and the new impurity phases appearing at 833°C. However, $LiMn_2O_4$ in this study exhibited

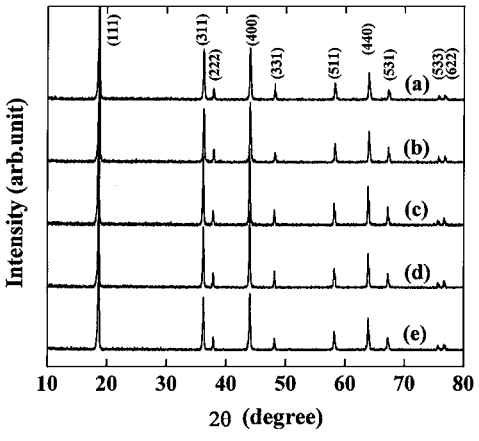

Fig. 1. X-ray diffraction patterns of $LiMn_2O_4$ powders calcined at various temperatures. (a) 700°C, (b) 750°C, (c) 800°C, (d) 850°C, and (e) 900°C.

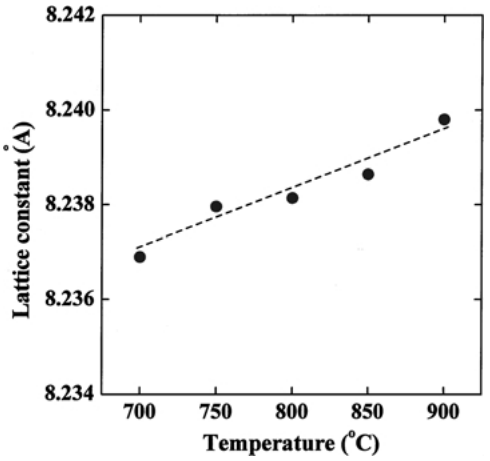

Fig. 2. Dependence of the average Mn oxidation state for the $LiMn_2O_4$ materials on the calcination temperatures.

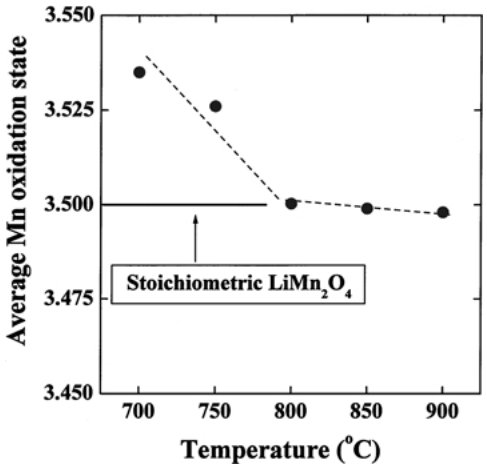

Fig. 3. Dependence of the lattice constants for the $LiMn_2O_4$ powders at various temperatures.

no concrete peak change or some impurities, such as tetragonal (I41/amd) phase until 900°C [16], although there was very small change of the ratio of (311)/(400) peaks.

Figure 2 shows the dependence of the lattice constants on the calcination temperatures. The lattice constants were determined by the Rietveld refinement of the XRD data. As shown in this figure, the lattice constant slightly increases from 8.237 Å to 8.240 Å with increasing calcination temperature from 700°C to 900°C. Because the ionic radius of Mn^{4+} (0.53 Å) is a smaller value than that of Mn^{3+} (0.65 Å), thus the lattice constant of the cubic unit cell calcined at high temperature is larger than that at lower temperatures.

The dependence of the average Mn oxidation state and the calcination temperatures is shown in Fig. 3. The lower calcination temperatures resulted in the formation of a more oxidized manganese ion because the manganese ion is stable preferentially as Mn^{4+} at lower temperatures. When the calcination temperatures increase, the amount of Mn^{4+} decreases by releasing oxygen which leads to a decrease in the average Mn oxidation state. Therefore, the average Mn oxidation state of $LiMn_2O_4$ spinel decreases as increasing calcination temperature. The $LiMn_2O_4$ material in this study shows the ideal stoichiometric value (Ave. Mn = 3.5) at 800°C.

Figure 4 shows the discharge capacities of the Li/1M $LiPF_6$-EC/DMC/$LiMn_2O_4$ cells with cycle number at a constant current density of 0.4 mA/cm^2 with a cut-off voltage of 3.0–4.3 V. The cycle characteristic of the

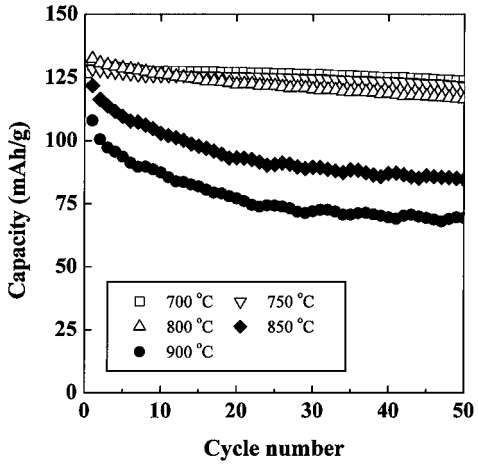

Fig. 4. Variation in specific discharge capacity with number of cycles for the Li/1M $LiPF_6$-EC/DMC/$LiMn_2O_4$ cells calcined at various temperatures.

$LiMn_2O_4$ cells could be divided into two groups during the cycling test. In the 4 V region, three cells calcined at low temperatures (700–800°C) showed fairly good cycling performances until 50 cycles. The cycle retention rates of these cells were 95.2%, 94.6%, and 87.9%, respectively. However, two $LiMn_2O_4$ cells calcined at higher temperatures (850–900°C) exhibited an abrupt capacity loss and very small discharge capacities after 50 cycles. The cycle retention rates of the two cells were 69.4% for the 850°C and 64.3% for the 900°C samples. Because the difference in cycle retention rate for the two groups was a very large value, it was assumed that

there are some important physicochemical changes in the $LiMn_2O_4$ structure; such as abrupt lithium sublimation, oxygen deficiency, and the ratio of Mn^{3+}/Mn^{4+}, due to the high calcination temperatures in air (850–900°C).

General reaction mechanism of $LiMn_2O_4$ could be proposed for the phase transformation or structural change, which resulted from the oxygen loss and lithium sublimation of $LiMn_2O_4$ material calcined at high temperatures (700–1100°C) [17, 18].

$$LiMn_2O_4(\text{cubic}) \rightarrow LiMn_2O_{4-z}(\text{cubic, oxygen deficiency}) + z/2O_2 \quad (1)$$

$$LiMn_2O_{4-z} + z/2O_2 \rightarrow Li_{1-2z'}Mn_{2-z'}O_{4-z-3z'-z''} \text{ (cubic/tetragonal, Li, O-deficiency)} + zLi_2MnO_3 + z''/2O_2 \quad (2)$$

$$Li_{1-2z'}Mn_{2-z'}O_{4-z-3z'-z''} + zLi_2MnO_3 + z''/2O_2 \rightarrow LiMnO_2(\text{orthorhombic}) + Mn_3O_4 \quad (3)$$

As shown above Eqs. (1)–(3), when $LiMn_2O_4$ spinel was calcined at higher temperatures, there are occurred many structural changes during calcinations process. Furthermore, this reaction mechanism suggested that the structural and electrochemical characteristics of $LiMn_2O_4$ were strongly resulted from the lithium and oxygen contents in the structure.

To reveal the reason of various cycle behaviors of $Li/LiMn_2O_4$ cells obtained at different calcination temperatures, it needs to investigate clearly these two factors, lithium amount and oxygen deficiency, as mentioned above. The lithium content in all resulting materials was analyzed with an inductively coupled plasma spectrometer (ICP, SPS7800, Seiko Instrument, Japan). Although similar investigations of oxygen effects of the $Li_{1+x}Mn_{2-x}O_4$ structure already reported by some research groups [18, 19], they did not suggest the quantitative data by oxygen analysis. Oxygen content in the spinel was measured quantitatively using an oxygen determination analyzer (RO-416DR, EF-40C, LECO Corporation, USA). It was used to investigate the oxygen deficiency on the electrochemical properties of the $LiMn_2O_4$ spinel [20].

Figure 5 exhibits the experimental procedure of oxygen analysis of $LiMn_2O_4$ material. This method could measure a real and exact oxygen content, regardless

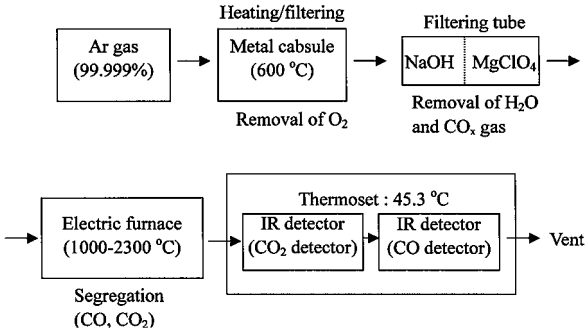

Fig. 5. Flow chart of oxygen analysis by oxygen determination analyzer.

of lithium content of the $LiMn_2O_4$ because measuring temperature is over 1600°C, which is about as much as two times higher than the starting temperature of lithium sublimation. It detected the oxygen amount in the CO and CO_2 gas after powder was calcined in the tin capsule at 1600°C. The change of oxygen content of resulting material can be explained in terms of oxygen loss during the calcination process. Such changes of oxygen should affect the composition and structural aspect of spinel compound to maintain the charge balance in the $LiMn_2O_4$ compound. We believe this is a very effective method to distinguish the oxygen content of the $LiMn_2O_4$ spinel which obtained at higher temperatures (≥850°C).

Table 1 shows the chemical analysis results of the $LiMn_2O_4$ spinel compounds, which were synthesized at higher temperatures (800, 850, and 900°C). As expected, there are a big difference in the lithium content between 800°C sample and other samples. The reason of different lithium amount in the resulting material is the fixed lithium amount in the starting materials, which investigate simultaneously the lithium effect as well as oxygen content. Although the lithium content of 800°C sample showed a large difference value compared to that of 850°C, the two samples calcined at 850°C and 900°C showed a similar lithium content each other. If the lithium sublimation at high temperature is the

Table 1. Chemical analysis of resulting $LiMn_2O_4$ materials obtained at different temperatures.

Temp. (°C)	Li (wt%)	Mn (wt%)	O (wt%)	2Li/Mn (mol/mol)
800	3.92	60.74	35.17	0.997
850	3.56	61.64	34.65	0.892
900	3.55	61.56	34.56	0.896

sole reason to induce a rapid capacity loss of $LiMn_2O_4$ cells (850–900°C), two materials should be indicated very similar cycle characteristics because the lithium content of these materials was the almost same. However, the discharge capacities of the two materials after 50 cycles were 84.6 mAh/g for the 850°C sample and 69.4 mAh/g for 900°C sample. It means that there may be another major effect to result in the capacity loss of Li/$LiMn_2O_4$ obtained between 850°C and 900°C samples.

Furthermore, oxygen analysis suggest one more interesting factor to us, which the oxygen amounts of resulting compounds continuously decrease, after abrupt decrease after 800°C, with increasing calcination temperature as shown in Table 1. In case of 950°C sample, which was not shown in this table because it contained many impurities in the XRD diagram, it had a larger oxygen decrease and showed a more serious capacity loss. This means that oxygen content (or deficiency) is also a very effective parameter to determining cycle performance of the $LiMn_2O_4$ spinel obtained at high temperatures.

In order to confirm the role of oxygen deficiency in different ways, the first charge/discharge curves of the Li/$LiMn_2O_4$cells obtained at various calcination temperatures were shown in Fig. 6. Wang et al. already reported that the synthesis of $LiMn_2O_4$ spinel with various oxygen content calcined at at 470°C and 530°C for 5 h in air, followed heating at various temperatures. They revealed that the oxygen deficient $LiMn_2O_4$ spinel exhibited a 4.4 V plateau ($C_{4.4\,V}$) and a 3.2 V plateau ($C_{3.2\,V}$) depending on the synthetic conditions [21]. As expected, two compounds obtained at 700°C and 750°C in this study showed no distinct plateaus except for the 4.0 V and the 4.15 V plateaus in the 4 V

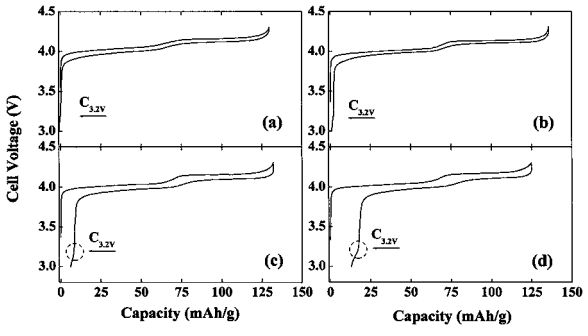

Fig. 6. The first charge/discharge curves for Li/1M $LiPF_6$-EC/DMC/$LiMn_2O_4$ cells calcined at various temperatures. (a) 750°C, (b) 800°C, (c) 850°C, and (d) 900°C.

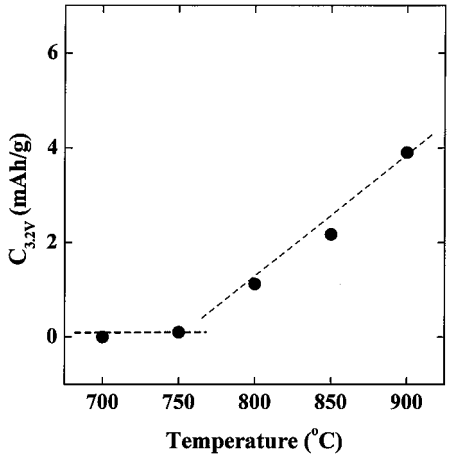

Fig. 7. Relation of between $C_{3.2\,V}$ and various calcination temperatures.

region. The absence of the plateau of 3.2 V at 700°C and 750°C may result from the oxygen rich state during pre-calcinations in oxygen atmosphere and fairly lower post-calcination temperatures in air atmosphere. However, the plateau of 3.2 V appeared in the samples obtained at more than 800°C and it suddenly increased as the calcination temperature increased. The dependence of the $C_{3.2\,V}$ and the calcination temperatures was shown in Fig. 7. The value of $C_{3.2\,V}$ was maintained steadily until 800°C, however, it increases suddenly with increasing calcination temperature. This result coincides with the oxygen analysis result as shown in Table 1. In other words, the calcination of $LiMn_2O_4$ at high temperature induces an oxygen deficiency in the spinel structure and the degree of oxygen deficiency in the spinel structure was represented by the scale of 3.2 V plateau in the charge/discharge curves. Therefore, the value of $C_{3.2\,V}$ could be an indicator for the oxygen deficiency degree in the $LiMn_2O_4$ spinel.

Based on these results, it was concluded that $LiMn_2O_4$ spinel powders with a high degree of oxygen deficiency exhibited even faster capacity fading rates and had a large $C_{3.2\,V}$ value. Therefore, we concluded that the oxygen deficiency and the lithium content were very important key parameters to improve battery performance of Li/$LiMn_2O_4$ system, especially, for the spinels obtained at the higher temperatures ($\geq$850°C).

Conclusion

$LiMn_2O_4$ has been synthesized at different calcination temperatures using the melt-impregnation method.

$LiMn_2O_4$ cells calcined at lower temperatures (700–800°C) showed excellent cycling performances at room temperature until 50 cycles. However, $LiMn_2O_4$ cells calcined at higher temperature (850–900°C) exhibited abrupt capacity loss and very small discharge capacities in the 4 V region. It resulted from lithium sublimation and oxygen deficiency of $LiMn_2O_4$ spinel structure over 800°C. We found that the 3.2 V plateau showed a very clear relation with the oxygen deficiency and represented the degree of oxygen deficiency in the spinel structure.

References

1. K. Mizushima, P.C. Jones, P.J. Wiseman, and J.B. Goodenough, *Mater. Res. Bull.*, **15**, 783 (1980).
2. C. Plichata, M. Salomon, S. Slane, M. Uchiyoma, B. Chua, W.B. Ebner, and H.W. Lin, *J. Power Sources*, **21**, 25 (1987).
3. J.R Dahn, U. Von Sacken, and C.A. Michel, *Solid State Ionics*, **44**, 87 (1990).
4. R.J. Gummow, D.C. Liles, and M.M. Thackeray, *Mater. Res. Bull.*, **28**, 1249 (1993).
5. T. Ohzuku, M. Kitagawa, and T. Hirai, *J. Electrochem. Soc*., **137**, 760 (1990).
6. W.J. Macklin, R.J. Neat, and R.J. Powell, *J. Power Sources*, **34**, 39 (1991).
7. V. Manev, A. Momchilov, A. Nassalevska, and A. Kozawa, *J. Power Sources*, **41**, 305 (1993).
8. D. Guyomard and J.M. Tarascon, *Solid State Ionics*, **69**, 222 (1994).
9. D.H. Jang, Y.J. Shin, and S.M. Oh, *J. Electrochem. Soc.*, **143**, 2204 (1996).
10. Y. Xia, Y. Zhou, and M. Yoshio, *J. Electrochem. Soc.*, **144**, 2593 (1997).
11. D. Guyomard and J.M. Tarascon, *J. Electrochem. Soc.*, **139**, 937 (1992).
12. M.M. Thackeray, Y. Shao-Horn, A.J. Kahaian, K.D. Kepler, E. Skinner, J.T. Vaughey, and S.A. Hackney, *Electrochem. & Solid-State Lett.*, **1**(1), 7 (1998).
13. Y. Xia, T. Sakai, T. Fujieda, X.Q. Yang, X. Sun, Z.F. Ma, J. McBreen, and M. Yoshio, *J. Electrochem. Soc.*, **148**, A723 (2001).
14. X.Q. Yang, X. Sun, M. Balasubramanian, J. McBreen, Y. Xia, T. Sakai, and M. Yoshio, *Electrochem. & Solid-State Lett.*, **4**(8), A117 (2001).
15. A. Yamada, K. Miura, K. Hinokuma, and M. Tanaka, *J. Electrochem. Soc*., **142**, 2149 (1995).
16. J.M. Tarascon, F. Coowar, G. Amatuci, F.K. Shokoohi, and D.G. Guyomard, *J. Power Sources*, **54**, 103 (1995).
17. S. Ma, Ph.D. dissertation, Saga University (2001).
18. J.M. Tarascon, W.R. Mckinnon, F. Coowar, T.N. Bowmer, G. Amatucci, and D. Guyomard, *J. Electrochem. Soc.*, **141**, 1421 (1994).
19. Yuan Gao and J.R. Dahn, *J. Electrochem. Soc.*, **143**, 100 (1996).
20. Y. Hideshima, Ph.D. dissertation, Saga University (2000).
21. X. Wang, Y. Yagi, Y.S. Lee, M. Yoshio, Y. Xia, and T. Sakai, *J. Power Sources*, **97/98**, 427 (2001).